EPR Spectroscopic Characterization of Neuronal NO Synthase†

Chris Galli,‡,§ Ryan MacArthur,‡ Husam M. Abu-Soud,|| Pamela Clark,|| Dennis J. Stuehr,*,||,⊥ and Gary W. Brudvig*,‡

Department of Chemistry, Yale University, 225 Prospect Street, New Haven, Connecticut 06511, Department of Immunology, Cleveland Clinic, Cleveland, Ohio 44195, and Department of Physiology and Biophysics, Case Western Reserve University, Cleveland, Ohio 44106

Received August 28, 1995; Revised Manuscript Received December 1, 1995⊗

ABSTRACT: Neuronal NO synthase (nNOS) consists of a reductase domain that binds FAD, FMN, NADPH, and calmodulin, and an oxygenase domain that binds heme, tetrahydrobiopterin, and the substrate L-arginine. One flavin in resting nNOS exists as an air-stable semiquinone radical. During NO synthesis, electron transfer occurs between the flavins and heme iron. We have characterized the nNOS heme iron and flavin semiquinone radical by electron paramagnetic resonance (EPR) spectroscopy. Under anaerobic conditions, the flavin radical spin relaxation was very slow (8 Hz at 22 K) and was enhanced 13-fold by dissolved dioxygen via spin−spin coupling. The flavin radical, probably the semiquinone $FMNH^{\bullet}$, was shown by progressive microwave power saturation and EPR saturation recovery under anaerobic conditions to be spin−spin coupled with the heme iron located in the nNOS oxygenase domain. Analysis of an nNOS preparation that was devoid of heme but contained the flavin radical revealed that spin−spin coupling increased the rate of flavin radical relaxation by a factor of 15. The presence of bound substrate (L-arginine) or the substrate analogue N^{ω}-nitro-L-arginine methyl ester (NAME) had no effect on the flavin spin relaxation kinetics. The observed g values of the nNOS heme were 7.68, 4.15, and 1.81 and were unchanged by occupation of the substrate binding site by L-arginine or NAME. The substrate also had no effect on the heme zero-field splitting parameter, $D = 5.2$ cm^{-1}. Together, the data indicate that the flavin and heme redox centers are positioned near each other in nNOS, consistent with their participating in an interdomain electron transfer. The flavin radical is affected by dissolved oxygen, suggesting that its binding site within the reductase domain is partially exposed to solvent, but is unaffected when substrate binds to the oxygenase domain. Substrate binding also appears to take place outside the first coordination shell of the nNOS heme iron.

The free radical nitric oxide (NO)[1] mediates a variety of physiological activities in the immune, circulatory, and central nervous systems of mammals (Nathan & Xie, 1994; Schmidt & Walter, 1994; Stuehr & Griffith, 1992). NO plays a role in the regulation of lymphocyte proliferation, the inhibition of platelet aggregation, and the control of vascular tone in tissue; in neuronal cells, the radical has been identified as a signal molecule in neurotransmission. Due in part to the diversity of cell types exhibiting NO synthesis, bioproduction of NO has attracted a great deal of recent attention. NO is formed in mammalian cells from the catalytic oxidation of L-arginine by three NO synthase (NOS) enzymes. An inducible isoform, such as murine macrophage NOS (iNOS), is expressed following induction by immunoactive cytokines such as interferon-γ or interleukin-1. The iNOS is always capable of NO synthesis, presumably due to its tightly bound calmodulin (CAM) prosthetic group. In contrast, two constitutive isoforms, such as rat neuronal NOS (nNOS) and endothelial NOS, are present continuously in an inactive form and require Ca^{2+}-promoted CAM binding to activate their NO synthesis. Binding of CAM to nNOS triggers electron transfer from the flavins to the heme catalytic center, reducing the ferric iron and initiating the subsequent oxygenase activity displayed by the NOS isoforms (Abu-Soud & Stuehr, 1993; Abu-Soud et al., 1994a, Matsuoka et al., 1994).

In spite of their differences in regulation, iNOS and nNOS have similar composition, in that both are bifunctional enzymes consisting of a reductase domain that binds CAM, FMN, FAD, and NADPH and an oxygenase domain that binds heme, tetrahydrobiopterin, and substrate L-arginine (Sheta et al., 1994; Ghosh & Stuehr, 1995). The NOS oxygenase domain is somewhat similar to another family of monooxygenase enzymes, the cytochrome P450s (cyt P450). The catalytic site of these enzymes is a redox active heme which binds dioxygen upon reduction to Fe(II). Cryogenic EPR and resonance Raman measurements of both resting

† This work was supported by the National Institute of Health Grants GM36442 (G.W.B.) and GM51491 (D.J.S.). D.J.S. is an Established Investigator of the American Heart Association.

* Corresponding authors: Dr. Dennis J. Stuehr, Immunology NN-1, Research Institute, Cleveland Clinic, 9500 Euclid Avenue, Cleveland, OH 44195; Fax: 216-444-9329; Dr. Gary W. Brudvig, Department of Chemistry, Yale University, 225 Prospect St., New Haven, CT 06511. Fax: 203-432-6144.

‡ Yale University.

§ Present address: Department of Chemistry, 221 Petty Building, University of North Carolina at Greensboro, Greensboro, NC 27412-5001.

|| Cleveland Clinic.

⊥ Case Western Reserve University.

⊗ Abstract published in *Advance ACS Abstracts,* February 1, 1996.

[1] Abbreviations: NO, nitric oxide; NOS, nitric oxide synthase; iNOS, inducible nitric oxide synthase; CAM, calmodulin; nNOS, neuronal NOS; cyt P450, cytochrome P450; NAME, N^{ω}-nitro-L-arginine methyl ester; ZFS, zero-field splittings; Arg-NOS, L-arginine-bound neuronal nitric oxide synthase; NAME-NOS, N^{ω}-nitro-L-arginine methyl ester-bound neuronal nitric oxide synthase; FAD, flavin adenine dinucleotide; FMN, flavin mononucleotide; ApoNOS, heme- and tetrahydrobiopterin-free neuronal nitric oxide synthase; NADPH, nicotinamide adenine dinucleotide phosphate.

0006-2960/96/0435-2804$12.00/0

nNOS and substrate-bound cyt P450 enzymes show that the heme is predominantly high-spin ferric, and five-coordinate, and has a cysteine thiolate as the proximal axial ligand. Substrate binding by nNOS and cyt P450 favors the high spin form of the ferric iron, and takes place above the plane of the heme in the distal pocket (Sato et al., 1976; Stuehr & Ikeda-Saito, 1992; Wang et al., 1993, 1994; Hu & Kincaid, 1991; Wells et al., 1992). In cyt P450, the three components of the heme transition $|5/2, -1/2\rangle > |5/2, +1/2\rangle$ show g values near 7.9, 3.7, and 1.7 (Sato et al., 1976). The spectroscopically well-characterized cyt P450 enzymes provide a model for the EPR characterization of the NOS heme pocket.

The NOS reductase domain is closely related to the redox-active NADPH cyt P450 reductase, which transfers electrons to the ferric heme of cyt P450 in a range of cell types and organisms. Both NOS and NADPH cyt P450 reductase contain one FAD and one FMN per subunit; in cyt P450 reductase, the O_2-stable free radical has been unambiguously identified as the FMN semiquinone (Otvos et al., 1986). The linear electron transfer sequence is NADPH → FAD → FMN → heme (Vermillion & Coon, 1978). The stable FMN semiquinone is also observed in the flavoprotein NADPH−sulfite reductase, where FMN cycles between the hydroquinone ($FMNH_2$) and the stable radical ($FMNH^{\bullet}$), while FAD is reduced almost exclusively to $FADH_2$ (Ostrowski et al., 1989). The O_2-stable free radical in NOS, presumably the semiquinone $FMNH^{\bullet}$, presents an ideal example whereby the flavin EPR signal can be used to study the location and orbital overlap of the flavin and heme. Recently, a field-swept EPR spectrum of NOS at 6 K displayed a sharp, $g = 2.00$ feature at 10 mW incident microwave power (Stuehr & Ikeda-Saito, 1992). As the intrinsic spin relaxation of flavin radicals is typically rather slow, this result is somewhat surprising: the EPR response of an isolated organic radical such as the flavin radical in NOS is expected to be severely saturated and power-broadened at this temperature and microwave power. The authors suggested the possibility that the spin relaxation of the radical is enhanced via spin−spin interactions with the heme iron. The flavin radical−heme iron spin−spin coupling, which in principle may contain dipolar and exchange components, is of interest regarding the enzyme's electron transfer pathway and mechanism.

In this paper, the spin−spin coupling between the flavin and heme centers of nNOS is examined via progressive microwave power saturation and EPR saturation recovery of the flavin radical. In addition, we use L-arginine and the substrate analogue N^{ω}-nitro-L-arginine methyl ester (NAME) to examine how binding site occupancy affects the nNOS flavin radical and heme iron environment. It has recently been demonstrated that NAME inhibits electron flux through nNOS by preventing flavin-mediated ferric heme reduction (Abu-Soud et al., 1994b). We therefore compared g values and zero-field (ZFS) splitting values of the L-arginine-bound (Arg−NOS) and NAME-bound (NAME−NOS) forms of nNOS.

MATERIALS AND METHODS

Samples of nNOS and apoNOS (heme-free nNOS) were prepared as previously described (Stuehr & Ikeda-Saito, 1992; Abu-Soud et al., 1994a,b). The samples used in the EPR study of the $F^{\bullet}$ radical and heme iron of NOS were 50−150 μM. The Arg−NOS sample contained 1 mM L-arginine. The NAME−NOS (NAME = N^{ω}-nitro-L-arginine methyl ester) sample contained 1 mM NAME. Substrate binding by NOS forces the heme iron to the high-spin state (Stuehr & Ikeda-Saito, 1992); neither the Arg−NOS nor the NAME−NOS sample displayed a low-spin heme EPR signal that is readily discernible in the field-swept EPR spectrum of a resting NOS sample that does not contain substrate or substrate analogue. The ApoNOS (heme-free nNOS) sample was treated with NADPH (40 mM HEPES, pH 7.4), approximately stoichiometric to flavin quantity, to prereduce the flavin radical. All NOS samples for EPR examination were prepared with 25% glycerol (v/v), a quantity shown to preserve protein structure in frozen samples (Hirsh et al., 1992a). Atmospheric dioxygen was removed from the protein sample for anaerobic measurements by repeatedly flushing a sealed EPR tube containing the sample with N_2, then rolling the solution to maximize exposure. Good reproducibility was observed with this method. Once brought to cryogenic temperatures, care was taken to eliminate freezing and thawing; when not in use, the NOS samples were stored at 77 K.

Progressive microwave power saturation measurements of the NOS flavin radical were made on an X-band EPR spectrometer designed for low-power sensitivity. The usable microwave power range of this spectrometer extends below 1 picowatt (Beck et al., 1991). The temperature of the samples, controlled by an Oxford ESR-900 cryostat, was measured by using a Si diode temperature sensor at the sample position. The microwave power incident at the sample position was calibrated by observing the signal intensity of a small capillary tube of MgO doped with Cr^{3+}. The capillary tube was placed inside a standard EPR sample tube containing the NOS protein. The EPR signal from the NOS flavin radical and the Cr^{3+} reference were then recorded in a single field-swept spectrum.

Saturation−recovery EPR measurements of the flavin radical in NOS were made on a home-built X-band pulsed EPR spectrometer as previously described (Beck et al., 1991). The transient spectra were recorded by tuning the external magnetic field to the zero crossing of the radical's first derivative spectrum (field position indicated by arrow in Figure 2). Saturation−recovery EPR signals were recorded without external field or microwave frequency modulation. Care was taken to ensure that the observed relaxation dynamics displayed no dependence on either the power or duration of the saturating pulse (Beck et al., 1991; Hirsh et al., 1992a). For each temperature, 10−20 recoveries of 500−5000 shots each were recorded at 4−7 different observation microwave powers. As the measured scalar component, k_{scalar}, of the saturation−recovery EPR signal of $F^{\bullet}$ displayed a weak dependence on observation microwave power (Beck et al., 1991), the zero-power linear extrapolation of k_{scalar} is reported.

The field-swept EPR spectra of the heme were recorded on a Varian E-line spectrometer. The sample temperature, controlled by an Oxford ESR-900 cryostat, was measured by a Si diode temperature sensor at the sample position. The g values of the heme in the NAME−NOS and Arg−NOS preparations were determined by recording the spectra of the NOS samples with an internal metmyoglobin standard ($g_{\perp} = 5.905$) (Aasa & Vänngård, 1975). A ~200 μM sperm whale (Sigma M-0380 used as received) myoglobin solution,

in 20 mM HEPES buffer at pH 7.0 with 30% glycerol (v/v), was placed in a small capillary tube that was inserted into a standard EPR tube containing the NOS protein. The $g_\perp = 5.905$ feature of the sperm whale myoglobin provides an ideal standard for the two lowest field transitions, g_x and g_y, of the NOS heme. The g_z value of the NOS heme was determined by using the NOS F$^\bullet$ signal ($g = 2.00$) as the reference.

The zero-field splittings of the heme in Arg−NOS and NAME−NOS were determined by measuring the integrated intensity of the lowest field Fe^{3+} transition (g_x) as a function of temperature. This transition presents the strongest and least obscured feature of the heme iron EPR spectrum. Typically 3−6 spectra at different microwave powers were recorded for each temperature; the integrated spectra were then averaged. Data points were obtained for approximately 40 temperatures over the range 4−95 K.

RESULTS

Progressive Microwave Power Saturation. Progressive microwave power saturation is a convenient method to determine relative spin relaxation rates. In this procedure, the doubly integrated area or the peak-to-trough height of the first derivative EPR signal is measured as a function of incident microwave power at a fixed temperature. The saturation curve is constructed by plotting the ratio of the signal amplitude to the square root of power versus the incident microwave power (Poole, 1983). The saturation data are fit to the expression (Beinert & Orme-Johnson, 1967):

$$S(P) = \left(1 + \frac{P}{P_{1/2}}\right)^{-b/2} \quad (1)$$

where S is the normalized EPR signal amplitude divided by the square root of the incident microwave power, and P is the incident microwave power. The two fitting parameters of the saturation curve are $P_{1/2}$, the power at which the signal attains half its unsaturated value, and b, the homogeneity parameter. The homogeneity parameter, b, traditionally ranges from $b = 3$ for a homogeneous transition (or Lorentzian line shape), to $b = 1$ for an inhomogeneous transition (or Gaussian line shape). In the unsaturated regime, $P \ll P_{1/2}$, the plot of S vs P is near linear with a slope of zero (see Figure 1). As the incident power is increased and P approaches $P_{1/2}$, the saturation curve displays nonlinear behavior, indicating the onset of saturation. The microwave power, $P_{1/2}$, is proportional to $(T_1T_2)^{-1}$, where T_1 is the spin−lattice relaxation time, and T_2 is the spin−spin relaxation time.

A spin accessing multiple relaxation channels via spin−spin coupling in addition to the spin−phonon-driven intrinsic recovery will display markedly different saturation properties, and a different $P_{1/2}$ value, compared to the isolated radical spin which is not spin−spin coupled. The NOS flavin radical spin can be isolated from radical−heme interactions by removing the heme prosthetic group containing the iron to form the ApoNOS. The saturation curve, and $P_{1/2}$ value, of the ApoNOS can be compared to the saturation curve of a heme-containing NOS to measure the effect of the heme on the flavin radical spin relaxation. The saturation curve, and the $P_{1/2}$ value of NAME−NOS, can be compared with the Arg−NOS progressive power saturation data to measure the effect of the substrate analogue NAME on the radical spin relaxation.

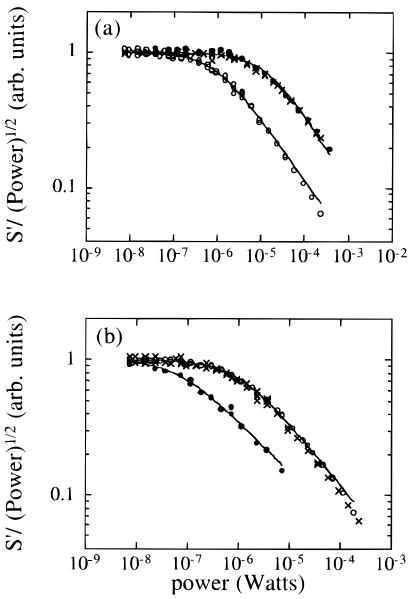

FIGURE 1: Progressive microwave power saturation of the NOS flavin radical. (a) The relaxation enhancement of the NOS flavin radical by O_2:aerobic Arg−NOS, solid circles; anaerobic Arg−NOS, open circles; Arg−NOS after reexposure to air, crosses; (b) In ApoNOS, which lacks the heme prosthetic group, the radical in anaerobic conditions saturates at ~1/15 the microwave power as that required for anaerobic Arg−NOS or NAME−NOS. Arg−NOS, open circles; NAME−NOS, crosses; ApoNOS, solid circles. The solid lines through the data points are fits of eq 1 to the data. Conditions: temperature, 6 K; field modulation frequency, 100 kHz; field modulation amplitude, 4 G; microwave frequency, 9.1 GHz. S' was taken as peak-to-trough amplitude of the flavin radical's EPR signal; identical results were obtained if S' was taken as the doubly integrated area.

However, intramolecular spin−spin coupling is not the only relaxation enhancement observed for the F$^\bullet$ radical of nNOS. Figure 1a displays the progressive power saturation data of the flavin radical of Arg−NOS under aerobic and anaerobic conditions. $P_{1/2}$ of the F$^\bullet$ radical is reduced approximately 13-fold by the removal of O_2 from the protein solution. The relaxation rate of the flavin is restored to the aerobic value by reexposing the sample to air. Similar effects were observed in the ApoNOS and NAME−NOS enzymes (data not shown). Apparently the paramagnetic triplet O_2, which can spin−spin couple with the flavin radical via exchange and dipolar mechanisms, has sufficient access to the radical to enhance the flavin spin relaxation.

A significant radical−heme spin−spin coupling is observed by progressive power saturation measurements of the proteins in the absence of O_2. The data are shown in Figure 1b. Clearly, the flavin radical of the ApoNOS protein saturates at a much lower incident power than do the Arg−NOS and NAME−NOS which contain the heme iron; Table 1a lists the $P_{1/2}$ values for anaerobic NAME−NOS, Arg−NOS, and ApoNOS. The flavin radical EPR g-values and lineshapes for ApoNOS, Arg−NOS, and NAME−NOS are indistinguishable, indicating that the removal of the noncovalently associated heme prosthetic group from the NOS protein does not significantly affect the flavin radical environment. In addition, the $P_{1/2}$ values for the radical F$^\bullet$ in NAME−NOS and Arg−NOS are identical within experimental error, indicating that the flavin radical's spin relaxation rate, at this temperature and pH, is not affected by the replacement of the physiological substrate L-arginine by NAME in the enzyme binding site. The $P_{1/2}$ of the F$^\bullet$ radical

Table 1

(a) Progressive Microwave Power Saturation of F• at 6 K

protein	$P_{1/2}$ (μW) (aerobic)	$P_{1/2}$ (μW) (anaerobic)
Arg−NOS	13 ± 2	0.9 ± 0.1
NAME−NOS	12 ± 1.5	1.0 ± 0.06
ApoNOS	0.71 ± 0.1	0.065 ± 0.010

(b) Saturation−Recovery EPR Measurements of Protein Radicals at 22 K

radical protein	k_{scalar} (Hz)	$k_{dipolar}$ (Hz)
F• Arg−NOS (anaerobic)	8	41
Y_D• of Mn-depleted PSII[a]	90	480

[a] From Koulougliotis et al. (1995).

is reduced approximately 15-fold by the removal of the heme from the protein. The difference in anaerobic $P_{1/2}$ values between the heme-containing NOS forms and the ApoNOS indicates there is a significant spin−spin coupling between the flavin radical and the heme iron.

It should be noted that progressive power saturation data characterized by a single $P_{1/2}$ is not strictly applicable to disordered samples of spins with pairwise dipolar coupling (Galli et al., 1996), as observed for the flavin radical F•−heme system in nNOS. The relaxation rate of a spin with dipolar coupling is a function of the angle θ between the external magnetic field and the interspin vector that joins the coupled spins. A progressive power saturation measurement of a disordered sample of such spins reflects a distribution in $P_{1/2}$ over θ because there is a distribution in T_1 over θ. However, an isotropic $P_{1/2}$ model is easily sufficient to distinguish the F• relaxation in the Arg−NOS and NAME−NOS with respect to the ApoNOS protein and to observe the effects of dioxygen on the flavin radical spin relaxation in aerobic versus anaerobic protein environments.

Saturation−Recovery EPR Spectroscopy. Relaxation enhancement of the flavin radical by the heme is also observed in the time domain via EPR saturation−recovery. This experiment measures the recovery of the sample magnetization following an excitation of the F• radical spin. The spin−lattice relaxation of anaerobic F• in the presence of the heme is non-single-exponential (Figure 2). Previous studies have shown that non-single-exponential spin−lattice relaxation is diagnostic of an orientation-dependent dipole−dipole interaction (Beck et al., 1991; Hirsh et al., 1992a,b; Koulougliotis et al., 1995). The relaxation enhancement of the flavin radical in NOS results from pairwise dipolar coupling between the radical and the heme iron. When an isotropic slow relaxing spin of Larmour frequency ω_s is coupled to an isotropic fast relaxing spin of frequency ω_f, the dipolar-driven recovery of the slow spin, $k_{dipolar}(\theta)$, is described by the "spectroscopic alphabet" expansion of Abragam (1961), and developed by Kukilov (1977), Hyde (1979), and Goodman (1985). The relaxation rate $k_{dipolar}(\theta)$ is a function of θ, the angle between the external magnetic field and the interspin vector **r** which joins the paramagnetic sites. For $(\omega_f - \omega_s)^2 \ll \omega_s$, $k_{dipolar}(\theta)$ is dominated by the B term of the spectroscopic alphabet (Hirsh et al., 1992a) and the θ dependence of $k_{dipolar}(\theta)$ is $k^B_{dipolar}(\theta)$ α $(1-3\cos^2\theta)^2$. In addition to the angular dependent rate $k^B_{dipolar}(\theta)$, the recovery of the slow-relaxing flavin radical also contains the spin-phonon-driven component of intrinsic recovery, k_i, and perhaps exchange-dependent relaxation, k_{ex}. If the exchange coupling is treated as isotropic, k_i and k_{ex} constitute the scalar

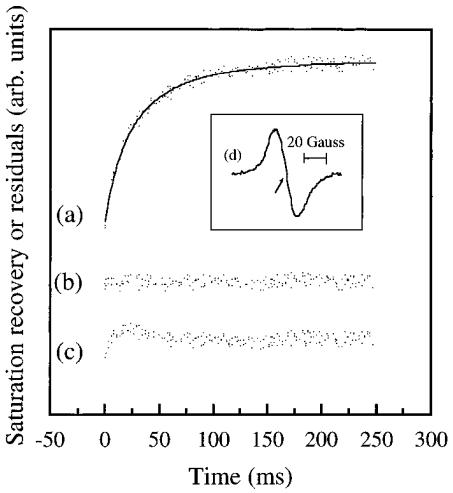

FIGURE 2: Saturation−recovery EPR transient of anaerobic Arg−NOS: (a) The experimental data points. The solid line through the data points is a fit of eq 2, which models the non-single-exponential transients in terms of a dipolar interaction between the flavin radical and heme (see text for details). The rate constants resulting from the fit, $k_{dipolar}$ and k_{scalar}, are given in Table 1b. (b) The residuals of the dipolar-model fit. (c) The residuals of a single-exponential fit. (d) The inset shows the field-swept EPR spectrum of the NOS flavin radical with an arrow indicating the experimental setting of the magnetic field for the saturation−recovery measurement. Saturation−recovery EPR conditions: temperature, 22 K; microwave frequency, 9.1 GHz; saturating pulse length, 100 ms; microwave observe power, 7 microwatts. Field-swept conditions: temperature, 22 K; field modulation frequency, 100 kHz; field modulation amplitude, 4 G; microwave power, 1 microwatt; microwave frequency, 9.1 GHz.

recovery rate k_{scalar}. The experimentally observed saturation-recovery EPR signal, $S(t)$, is then given by

$$S(t) = 1 - N\int_0^{\pi}(\sin\theta)e^{-(k^B_{dipolar}(\theta)+k_{scalar})t}d\theta \qquad (2)$$

where N is a normalization constant. The solid line through the data points in Figure 2 is a fit of eq 2 to the data; the fit results in the rate constants $k^B_{dipolar}$ and k_{scalar} given in Table 1b for the spin−lattice relaxation of the flavin radical in anaerobic Arg−NOS.

The spin relaxation of the flavin radical in anaerobic Arg−NOS is multicomponent because the organic radical spin is coupled to the heme iron via dipolar coupling. Exchange coupling between the spins may also provide a recovery channel for the flavin radical. While a complete description of the spin−spin coupling between the flavin radical and the heme iron must include the anisotropy of the heme iron that arises from ZFS, the current isotropic-limit model sufficiently quantifies the non-single-exponential kinetics.

Zero-Field Splittings. The heme iron of neuronal NOS has a similar overall ligand environment and shares optical and EPR spectroscopic similarities with the heme iron of the cytochrome P450s (McMillian et al., 1992; Stuehr & Ikeda-Saito, 1992; Wang et al., 1993). As mentioned, the NOS heme iron is bound to the protein by a cysteine thiolate ligand and is predominantly five coordinate and high spin in the ferric form (McMillian et al., 1992; Stuehr & Ikeda-Saito, 1992; Wang et al., 1993). Saturation of the heme iron L-arginine binding site, as in the present work, ensures the high-spin form of the iron. High-spin Fe^{3+} is an $S = 5/2$ spin state in which the components $M_s = \pm 1/2, \pm 3/2, \pm 5/2$ are degenerate. However, the degeneracy between the

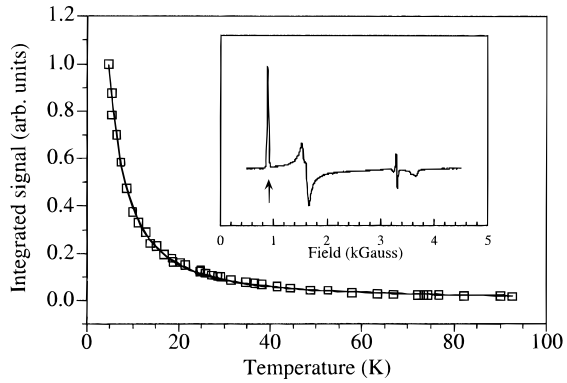

FIGURE 3: Determination of the heme iron zero-field splitting in NOS. The open squares are the integrated signal intensities of the heme iron g_x transition in Arg−NOS. The solid line through the data points is a fit to the data of eq 3, which yields the zero-field splitting parameter D (see Table 2). Conditions: field modulation frequency, 100 kHz; field modulation amplitude, 20 G; microwave power, 1−190 mW; microwave frequency, 9.3 GHz. The inset shows the field-swept EPR spectrum of Arg−NOS with an arrow denoting the g_x transition. Conditions: temperature, 6 K; field modulation frequency, 100 kHz; field modulation amplitude, 20 G; microwave frequency, 9.3 GHz; microwave power, 10 mW.

doublets is lifted when the ligand field has less than cubic symmetry. This zero-field splitting, i.e., the difference in energy between the doublet components of the $S = 5/2$ state in the absence of an external magnetic field, is important for two reasons: (1) the zero-field splitting reports on the coordination environment of the heme iron, and (2) the internal magnetic fields associated with the heme may be large relative to the externally applied magnetic field. The latter is important with regard to quantifying the spin−spin coupling between the ferric spin and the spin of the flavin radical.

The zero-field splittings of the heme in Arg−NOS and NAME−NOS were determined by measuring the integrated intensity of the heme iron g_x EPR transition as a function of temperature. As only the $|5/2, -1/2\rangle \rightarrow |5/2, +1/2\rangle$ transition is observed in this EPR experiment, populations in the $M_s = \pm 3/2, \pm 5/2$ doublets reduce the signal intensity of the observed transition. The heme iron of NOS is a spin with one unique axis created by the cysteine thiolate axial ligation. The inequivalency of the heme plane axes, say x and y, is in general expressed in a rhombic distortion parameter E. The magnitude of the rhombic parameter E can be estimated from the observed g values of the heme iron (Sato et al., 1976). As this analysis for the heme iron of NOS shows E to be relatively small with respect to the zero-field parameter D, $E/D \sim 0.1$, it is not necessary to include the xy inequivalency. E/D for the NOS heme iron is smaller than the presented experimental uncertainty in D.

Figure 3 displays, as a function of temperature, the integrated intensity of the NOS g_x heme iron transition in Arg−NOS. (This transition is indicated by the arrow in the inset of Figure 3). The open squares are the data points. The solid line through the data points is a fit of

$$S(T) = \frac{N(1 - e^{-\theta/T})}{1 + e^{-\theta/T} + e^{-(2D-\theta)/T} + e^{-2(D+\theta)/T} + e^{-2(3D-\theta)/T} + e^{-3(2D+\theta)/T}} \quad (3)$$

where $S(T)$ is the integrated EPR signal intensity, θ is the Zeeman splitting $h\nu/k_B = 0.44$ K, D is the zero-field splitting parameter, and N is an overall scale factor. When D is positive, the doublet $|5/2, \pm 3/2\rangle$ lies $2D$ above the ground-state doublet $|5/2, \pm 1/2\rangle$, and the doublet $|5/2, \pm 5/2\rangle$ lies $4D$ above the $|5/2, \pm 3/2\rangle$ doublet in the absence of an external magnetic field.

The zero-field splitting parameter, D, and the g values g_x, g_y, and g_z, have been determined for the heme iron of Arg−NOS and NOS−NAME; the results are given in Table 2. The zero-field splitting parameter D, as well as g_x and g_z, are essentially the same for the heme irons, indicating that the presence of NAME does not significantly alter the first ligation sphere of Fe^{3+}.

DISCUSSION

The catalytic center of nNOS contains the heme and substrate binding sites. We have probed the heme environment and ligation by measuring the g values and zero-field splittings of the heme iron via field-swept EPR. The observed g values 7.68, 4.15, and 1.81, shown in Table 2, are virtually identical for the substrate-free NOS (Stuehr & Ikeda-Saito, 1992), Arg−NOS, and NAME−NOS. The small differences noted for the $g = 4.15$ transition probably arise from errors caused by an interfering EPR signal from rhombic iron (Stuehr & Ikeda-Saito, 1992) rather than from real variations of g_y. Apparently the substrate is neither directly ligated to the heme iron nor sufficiently close to perturb the heme environment with respect to the substrate-free protein structure. That the substrate binding site is removed from the heme iron is also demonstrated by the equivalency of the zero-field splittings measured in the Arg−NOS and NAME−NOS proteins (see Table 2). If the substrate binding appreciably altered the heme environment, the effect would be observed as a different ZFS for NAME with respect to L-arginine. The separation of substrate binding site and heme environment is also observed in the oxygenase cyt $P450_{cam}$ (EC 1.14.15.1), where the bound substrate, 2-bornanone, is oriented so as to contact the activated dioxygen (Poulos et al., 1985) but lies well outside the ferric ligation sphere. The nNOS heme is somewhat distinguished from the cyt P450 heme, however, as both the g values and the ZFS differ slightly. Table 2 also shows the ZFS and g values for nNOS, for two of the better characterized cyt P450s, cyt $P450_{cam}$ (Tsai et al., 1970) and cyt P450 of rabbit liver microsomes (Peisach & Blumberg, 1970), and for three model heme−thiolate complexes (Tang et al., 1976). There is a general trend of increasing values of D as the rhombicity of the EPR signal decreases, with the values for nNOS falling between those of the cyt P450s and the model heme−thiolate complexes. A significant factor may be the Fe−S bond length which determines the extent of interaction of the sulfur and iron valence orbitals and is about 0.1 Å longer in the model heme−thiolate complex (Tang et al., 1976) than in cyt $P450_{cam}$ (Poulos et al., 1987). Therefore, the differences in g values and D of nNOS from those of cyt $P450_{cam}$ may be due to a slightly longer Fe−S bond in nNOS.

While the EPR spectrum of free flavin semiquinones may exhibit hyperfine structure (Ehrenberg, 1962), spectral inhomogeneity in protein-bound flavin radicals obscures this interaction. The typical flavoprotein radical signal in a smooth, structureless Gaussian of ~20 G line width (Beinert

Table 2: *g* Values and Zero-Field Splittings of the NOS and cyt P450 Hemes

sample	D (cm^{-1})	g_x	g_y	g_z
substrate-free NOS (Stuehr & Ikeda-Saito, 1992)	na	7.68	4.12	1.81
Arg−NOS	5.4 ± 0.8	7.68	4.15	1.81
NAME−NOS	5.1 ± 0.7	7.68	4.16	1.81
cyt $P450_{cam}$ (*P. putida*) (Tsai et al., 1970)	3.8	8.0	4.0	1.8
cyt P450 rabbit liver microsomes (Peisach & Blumberg, 1970)	3.95	8.08	3.68	1.71
Fe(P)(SPh)[a] (Tang et al., 1976)	na	7.2	4.7	1.9
Fe(PPIXDME)(SC_6H_4Cl)[a] (Tang et al., 1976)	na	7.2	4.8	1.9
Fe(PPIXDME)($SC_6H_4NO_2$)[a] (Tang et al., 1976)	8−10	na	na	na

[a] P = octaethylporphyrin; PPIXDME = protoporphyrin IX dimethyl ester.

& Orme-Johnson, 1967), as observed for the $FMNH^\bullet$ radicals of NADPH−cytP450 reductase (Iyanagi & Mason, 1973) and NADPH−sulfite reductase (Ostrowski et al., 1989). The $F^\bullet$ radical spectrum of nNOS is no exception; the transition is well fit by a Gaussian of width 21 G for the temperatures examined (4−58 K). This line shape and width display no dependence on substrate, consistent with the L-arginine and flavin binding sites being located in separate domains of nNOS (Sheta et al., 1994).

The progressive microwave power saturation data for $F^\bullet$ show the flavin radical is spin−spin coupled to both dissolved dioxygen and the NOS heme. The spin relaxation enhancement of $F^\bullet$ by dioxygen indicates that the radical flavin binding site of nNOS is accessible to small molecules in solution. The appreciable magnitude of the dioxygen effect is due, at least in part, to the slow intrinsic spin relaxation of the flavin radical $F^\bullet$, given in Table 1b at 22 K. For comparison, also shown in Table 1b are the spin-relaxation rates, $k^B_{dipolar}$ and k_{scalar}, for the tyrosine radical, $Y_D^\bullet$, of photosystem II at 22 K. The intrinsic spin relaxation, k_{scalar}, of the nNOS flavin radical $F^\bullet$ is about an order of magnitude slower than that observed for the tyrosine radical at this temperature. One explanation for the slow intrinsic spin relaxation of $F^\bullet$ is the weak hyperfine interaction, as evidenced by its featureless field-swept spectrum. A correlation between k_{scalar} and the magnitude of the hyperfine splitting for tyrosine radicals has previously been noted (Galli et al., 1995). The spin−lattice relaxation of $F^\bullet$ in nNOS is so slow at this temperature that O_2 provides a significant relaxation pathway. The relaxation enhancement of $F^\bullet$ by O_2 increases the $P_{1/2}$ by a factor of ∼13 over the anaerobic value (see Figure 1a), while the spin−lattice relaxation of $Y_D^\bullet$ is not affected by the presence of O_2 (Beck and Brudvig, unpublished results). The difference between $F^\bullet$ in NOS and $Y_D^\bullet$ in photosystem II is due, at least in part, to their different intrinsic spin−lattice relaxation rates. Because of the faster relaxation of $Y_D^\bullet$, it is less affected by the additional relaxation pathway provided by O_2. However, $Y_D^\bullet$ is buried in photosystem II approximately 25 Å from the nearest protein surface (Innes & Brudvig, 1989) and may not be as accessible to O_2. The greater effect of O_2 on the spin relaxation of $F^\bullet$ in NOS is consistent with an exposed binding site for the flavin in nNOS.

The removal of dissolved dioxygen from the protein solution allows the flavin radical $F^\bullet$−heme spin−spin interaction to be observed without interference. The radical−heme spin−spin interaction causes a 15-fold enhancement of the flavin radical's spin relaxation (Figure 1b) and also gives rise to the observed non-single-exponential spin−lattice relaxation of anaerobic Arg−NOS at 22 K (Figure 2).

The substrate analogue NAME has been observed to inhibit the reduction of the nNOS heme iron by the flavins; NAME also inhibits dithionite reduction of the ferric heme (Abu-Soud et al., 1994b). However, NAME in the substrate binding site alters neither the *g* values nor ZFS of the heme with respect to the physiological substrate L-arginine. As the immediate heme environment is not affected by the substrate or NAME, perhaps the inhibition of heme reduction is of electrostatic origin. NAME contains a nitro group not found in L-arginine and thus has distinct charge distributions that could result in significantly different reduction potentials of the heme (Varadarajan et al., 1989). NAME's inhibition of flavin-mediated heme reduction is currently being employed to study if changes in the $F^\bullet$−heme coupling occur upon binding of CAM to nNOS.

ACKNOWLEDGMENT

We thank Drs. David Bredt and Solomon Snyder for the cells used to generate nNOS and Drs. Masao Ikeda-Saito and Jack Lancaster for helpful early discussions.

REFERENCES

Aasa, R., Vänngård, T. (1975) *J. Magn. Reson. 19*, 308−315.
Abu-Soud, H. M., & Stuehr, D. J. (1993) *Proc. Natl. Acad. Sci. U.S.A. 90*, 10769−10772.
Abu-Soud, H. M., Yoho, L. L., & Stuehr, D. J. (1994a) *J. Biol. Chem. 269*, 32047−32050.
Abu-Soud, H. M., Feldman, P. L., Clark, P., & Stuehr, D. J. (1994b) *J. Biol. Chem. 269*, 32318−32326.
Abragam, A. (1961) *The Principles of Nuclear Magnetism*, Clarendon Press, Oxford.
Beck, W. F., Innes, J. B., Lynch, J. B., & Brudvig, G. W. (1991) *J. Magn. Reson. 91*, 12−29.
Beinert, H., & Orme-Johnson, W. H. (1967) in *Magnetic Resonance in Biological Systems* (Ehrenberg, A., Malmström, B. G., & Vänngård, T., Eds.) pp 221−247, Pergamon Press, Oxford.
Ehrenberg, A. (1962) *Ark. Kemi 19*, 97−117.
Galli, C., Atta, A., Andersson, K. K., Gräslund, A., & Brudvig, G. W. (1995) *J. Am. Chem. Soc. 117*, 740−746.
Galli, C., Innes, J. B., Hirsh, D. J., & Brudvig, G. W. (1996) *J. Magn. Reson.* (in press).
Goodman, G., & Leigh, J. S., Jr. (1985) *Biochemistry 24*, 2310−2317.
Hirsh, D. J., Beck, W. F., Innes, J. B., & Brudvig, G. W. (1992a) *Biochemistry 31*, 532−541.
Hirsh, D. J., Beck, W. F., Lynch, J. B., Que, L. J., & Brudvig, G. W. (1992b) *J. Am. Chem. Soc. 114*, 7475−7481.
Hu, S., & Kincaid, J. R. (1991) *J. Am. Chem. Soc. 113*, 9760−9766.
Hyde, J. S., Swartz, H. M., & Antholine, W. E. (1979) in *Spin Labelling II: Theory and Applications* (Berliner, L. J., Ed.) pp 71−113, Academic Press, New York.
Innes, J. B., & Brudvig, G. W. (1989) *Biochemistry 28*, 1116−1125.
Iyanagi, T., & Mason, H. S. (1973) *Biochemistry 12*, 2297−2308.

Koulougliotis, D., Tang, X., Diner, B. A., & Brudvig, G. W. (1995) *Biochemistry 34*, 2850−2856.
Kulikov, A. V., & Likhtenshtein, G. I. (1977) *Adv. Mol. Relax. Interact. Processes 10*, 47−79.
Matsuoka, A., Stuehr, D. J., Olson, J. S., Clark, P., & Ikeda-Saito, M. (1994) *J. Biol. Chem. 269*, 20335−20339.
McMillian, K., Bredt, D. S., Hirsch, D. J., Snyder, S. H., Clark, J. E., & Masters, B. S. S. (1992) *Proc. Natl. Acad. Sci. U.S.A. 89*, 11141−11145.
Nathan, C. F., & Xie, Q.-w. (1994) *Cell 78*, 915−918.
Ostrowski, J., Barber, M. J., Rueger, D. C., Miller, B. E., Siegel, L. M., & Kredich, N. M. (1989) *J. Biol. Chem. 264*, 15796−15808.
Otvos, J. D., Krum, D. P., & Masters, B. S. S. (1986) *Biochemistry 25*, 7220−7228.
Peisach, J., & Blumberg, W. E. (1970) *Proc. Natl. Acad. Sci. U.S.A. 67*, 172−179.
Poole, C. P. (1983) *Electron Spin Resonance. A Comprehensive Treatise on Experimental Techniques*, John Wiley and Sons, New York.
Poulos, T. L., Finzel, B. C., Gunsalus, I. C., Wagner, G. C., & Kraut, J. (1985) *J. Biol. Chem. 260*, 16122−16130.
Poulos, T. L., Finzel, B. C., & Howard, A. J. (1987) *J. Mol. Biol. 195*, 687−700.
Sato, M., Rispin, A. S., & Kon, H. (1976) *Chem. Phys. 18*, 211−224.
Schmidt, H. H. H. W., & Walter, U. (1994) *Cell 78*, 919−925.
Sheta, E. A., McMillan, K., & Masters, B. S. S. (1994) *J. Biol. Chem. 269*, 15147−15153.
Stuehr, D. J., & Griffith, O. W. (1992) *Adv. Enzymol. Relat. Areas Mol. Biol. 65*, 287−346.
Stuehr, D. J., & Ikeda-Saito, M. (1992) *J. Biol. Chem. 267*, 20547−20550.
Tang, S. C., Koch, S., Papaefthymiou, G. C., Foner, S., Frankel, R. B., Ibers, J. A., & Holm, R. H. (1976) *J. Am. Chem. Soc. 98*, 2414−2434.
Tsai, R., Yu, C. A., Gunsalus, I. C., Peisach, J., Blumberg, W. E., Orme-Johnson, W. H., & Bienart, H. (1970) *Proc. Natl. Acad. Sci. U.S.A. 66*, 1157−1163.
Varadarajan, R., Zewart, T. E., Gray, H. B., & Boxer, S. B. (1989) *Science 243*, 69−72.
Vermillion, J. L., & Coon, M. J. (1978) *J. Biol. Chem. 253*, 8812−8819.
Wang, J., Stuehr, D. J., Ikeda-Saito, M., & Rousseau, D. L. (1993) *J. Biol. Chem. 268*, 22255−22258.
Wang, J., Rousseau, D. L., Abu-Soud, H. M., & Stuehr, D. J. (1994) *Proc. Natl. Acad. Sci. U.S.A. 91*, 10512−10516.
Wells, A. V., Li, P., Champion, P. M., Martinis, S. A., & Sligar, S. G. (1992) *Biochemistry 31*, 4384−4393.

BI9520444